Stoichiometric Analysis of Ammonium Nitrate and Ammonium Perchlorate with Nanosecond Laser Induced Breakdown Spectroscopy

S. Sreedhar, S. Venugopal Rao,[a] P. Prem Kiran, Surya P. Tewari, and G. Manoj Kumar

Advanced Centre of Research in High Energy Materials **(ACRHEM)**
University of Hyderabad, Hyderabad 500046, India.

a Author for correspondence e-mail: svrsp@uohyd.ernet.in

ABSTRACT

We present our results on the stoichiometric analysis of ammonium nitrate (AN) and ammonium Perchlorate (AP) studied using laser induced breakdown spectroscopy (LIBS) with nanosecond pulses. The LIBS spectra collected for AP and AN, without any gating and using a high resolution spectrometer, exhibited characteristic lines corresponding to O, N, H, C, and K. The Oxygen line at 777.38 nm and three Nitrogen lines (N_1, N_2, N_3) at 742.54 nm, 744.64 nm, 747.12 nm were used for evaluating the Oxygen/Nitrogen ratios. The intensities were calculated using area under the peaks and normalized to their respective transition probabilities and statistical weights. The O/N_1 ratios estimated from the LIBS spectra were ~4.94 and ~5.11 for AP and O/N_3 ratios were ~1.64 and ~1.47 for AN obtained from two independent measurements. The intensity ratios show good agreement with the actual stoichiometric ratios - four for AP and one for AN.

Key words: Ammonium Nitrate, Ammonium Perchlorate, High Energy Materials, LIBS, nanosecond.

1. INTRODUCTION

Laser Induced Breakdown Spectroscopy (LIBS) is a prominent technique for detection and analysis of chemical, biological, explosive, and hazardous materials. LIBS involves interaction of a target with an intense laser pulse which generates plasma. The spectral emission from the plasma contains specific signature of atoms of the material [1-3]. The emission wavelength depends on specific atoms/ions while the intensity is proportional to their density. LIBS offers several advantages compared to other spectroscopic techniques including (a) Less sample preparation time (b) Simultaneous multiple element analysis for almost all the elements in the periodic table (c) Real-time response (d) Any sample format – solid, liquid or gas (e) Requirement of tiny amount of sample and (f) High sensitivity [4]. This technique has now been widely used to study various materials including metals, alloys, biological samples, polymers, soil, environmental pollutants, land mines, and explosive materials to name a few [5-19]. LIBS technique is particularly attractive for the detection of high energy materials (HEM's) due to its stand-off detection capability, requirement of minute quantities of material, and rapid detection. A number of HEM's including TNT, RDX, HMX, and PETN have been studied using LIBS [20-24]. Stand-off detection of explosives up to 50 meters range has also been achieved recently [25-28]. Majority of energetic materials are composed of hydrogen, carbon, oxygen, and nitrogen, and therefore the task of categorizing a HEM from others using LIBS data becomes unwieldy. Moreover, the contribution towards the peaks in LIBS spectra from the ambient air makes the task much more intricate. It requires careful analysis of the data to conclude whether given material is HEM or not and more importantly the exact identification of the HEM. One approach to circumvent this problem is to purge the sample chamber with an inert gas like argon but in a standoff system this cannot be implemented. Recent studies proved that it is possible to reduce these affects by a dual pulse technique [29-30]. Significantly, it was reported that intensity ratios of the various lines combined with the different statistical analysis is a useful method for discrimination of the HEMs [22,24]. Rai et al [31] have characterized the organic compounds 4-nitroaniline and 4-nitrotoluene by measuring the intensity of atomic lines. They inferred that the O(771.1)/N(744.2) intensity ratio is a unique parameter to discriminate each nitro-compound from the explosives. Díaz et al. [32] have demonstrated that LIBS has the ability to identify the presence of AN based on H_α (656.3 nm) and H_β (486.1 nm) emission lines. In this paper we present our results on LIBS studies of Ammonium Nitrate (AN), Ammonium Perchlorate (AP) excited with ns pulses. From the Oxygen/Nitrogen line ratios we calculated the

Chemical, Biological, Radiological, Nuclear, and Explosives (CBRNE) Sensing XI, edited by Augustus Way Fountain III, Patrick J. Gardner, Proc. of SPIE Vol. 7665, 76650J · © 2010 SPIE · CCC code: 0277-786X/10/$18 · doi: 10.1117/12.850014

stoichiometric ratios, which were in excellent agreement with the actual stoichiometric values. The advantage in our case is that the LIBS data obtained were non-gated. The spectra were recorded with (1) Bare sample in air and (2) Sample + KBr pellet. AP and AN belong to an important class of HEM's extensively used as oxidizers in rocket propellants and improvised explosive devices.

2. EXPERIMENTAL DETAILS

Figure 1 illustrates the schematic of experimental set up used for recording the LIB spectra. Second harmonic of a Nd :YAG laser operating at **532 nm** and delivering **7 ns, 10 Hz** pulses was used for all the experiments. The input beam diameter was **~6.5 mm** and pulses with a typical energy of **~25 mJ** were focused using an 80 mm lens on to the sample. The Rayleigh range was estimated to be ~0.5 mm. The beam waist at focus was estimated to be ~20 μm, corresponding to a peak intensity of >200 GW/cm^2. The sample was placed approximately 1 mm before the focus (towards the lens) where the spot size was estimated to be ~80 μm and the peak intensity ~18 GW/cm^2. As the laser energy increased we observed light and sound coming from the focal region beyond the breakdown threshold of material. The breakdown threshold for AN + KBr and AP + KBr was estimated at ~1.06 GW/Cm^2. The LIBS data was recorded with bare samples as well as samples made into pellets with KBr. As the experiment was executed in ambient air it was essential to avoid the contribution of LIBS signal from air. The breakdown threshold of air (>100 GW/cm^2) was well above the breakdown threshold for AP/AN in KBr matrix. The light from the breakdown region was collected using collection lenses of 100 mm and 150 mm placed 30° to the propagation direction, which in turn was connected to a fiber and a spectrometer (USB 4000 from Ocean Optics; 350-1050 nm). The resolution of spectrometer was ~1.5 nm. The data was collected with a 1000 ms integration time.

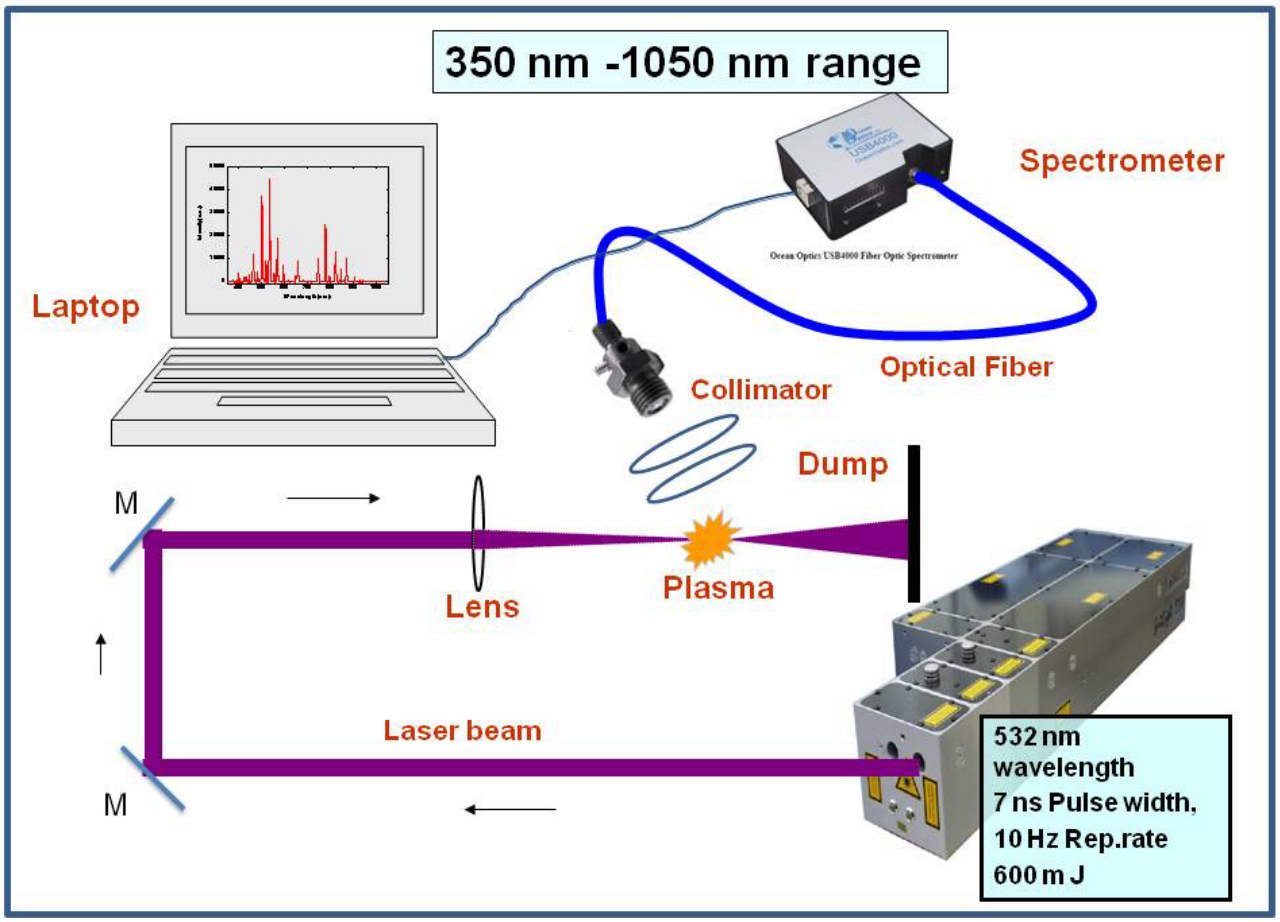

Figure 1 Experimental setup used for collecting LIBS spectra using ns pulses.

3. RESULTS AND DISCUSSION

Figures 2 (a) – (d) illustrate the detailed LIBS spectra of AP and AN. We observed a strong continuum since the data was collected without any gating facility. The spectra have been corrected for continuum background using a simple Matlab program. Each spectrum is split into two spectral regions (350 – 550 nm and 550 – 900 nm) for clarity and it is evident that all the spectra consist of several discrete peaks. These peaks have been assigned to different neutral and ionic states using the NIST database [33]. Both AP and AN spectra contained lines corresponding to Nitrogen (747.12 nm, 819.53 nm, and 868.61 nm), Oxygen (777.38 nm, 844.8 nm) and Hydrogen (656.4 nm). AP spectra exhibited the Cl lines at 382.04 nm, 438.15 nm, and 481.6 nm. We have also observed lines corresponding to K (694.04nm, 766.6nm, 770.05nm) and Na (589.11nm) in both the spectra. K lines are from the KBr matrix and Na could be an impurity either in KBr or the compound itself. We have observed the ionic lines for N^{3+}(374.36 nm), N^{2+}(393.21 nm), N^{+}(396.84 nm, 399.5 nm, 500.2 nm, 567.16 nm) in both AP and AN spectra. These lines were not observed when the spectrum for air/KBr was recorded separately indicating that these lines were exclusively from AP and AN samples. The LIBS signal was strong and we could register decent number of counts in the spectrometer even for input pulse energies <10 mJ.

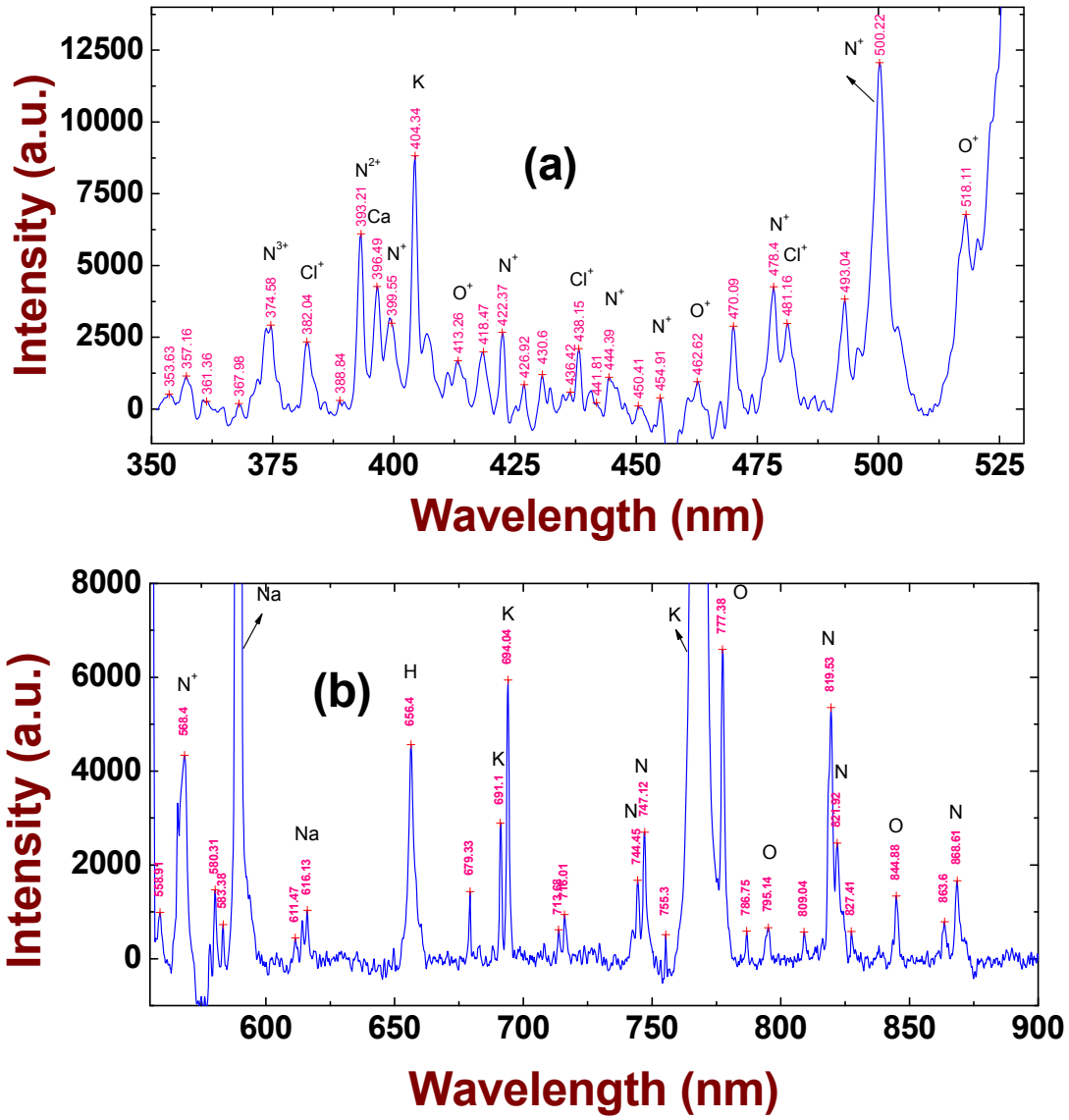

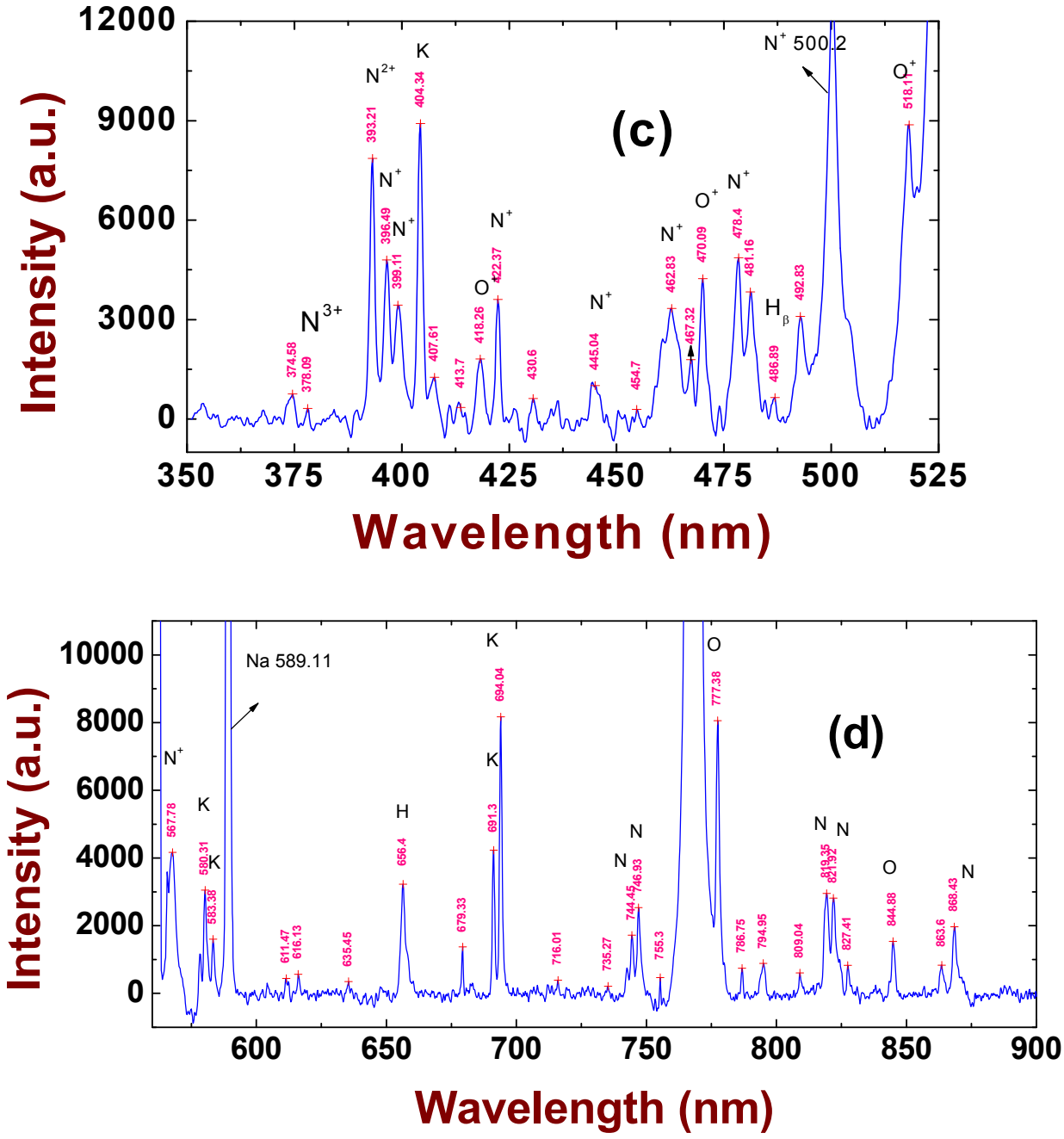

Figure 2 LIBS spectra of (a) AP between 350 nm- 550 nm, **(b)** AP between 550-900 nm, **(c)** AN between 350 -525 nm and **(d)** AN between 550 – 900 nm

Tables 1 and 2 show the detailed assignment of all the peaks observed in (a) ambient air, (b) pure KBr pellet, (c) AP/AN + KBr pellets. LIBS spectra for AP and AN were collected from three independent measurements and data is shown in both the tables. The underlined data in tables indicate the peaks exclusive for that particular compound. Most of the peaks observed were assigned to the elemental peaks with assistance from NIST database. Small changes (<0.1 nm) in the peak positions could be due to the calibration errors from our spectrometer.

AIR	KBr	AN (NH_4NO_3)			Element (NIST)
		Trial 1	Trial 2	Trial 3	
		374.58	374.58	374.58	N^{3+} (374.75), O3+(374.48),
				384.24	O+ (384.28, 384.35, 384.78)
		393.21	393.21	393.21	N^{2+} (393.85)
			396.93	396.93	N^{+} (395.58)
399.33	399.11				N^{+} (399.5), N^{2+} (399.86)
	404.34	404.34	404.34	404.34	N2+ (?), O+
	413.26		413.26	413.26	O+ (413.28)
	418.26	418.26	418.47	418.26	O+ (418.54, 418.97)
424.32	422.59	422.59	422.37	422.37	N+ (422.77)
	430.6		430.6	430.6	
			436.42	436.42	O+ (436.68), O+ (436.82)
444.39	444.39	446.11	444.39	444.39	O+ (444.7, 444.8), N+ (444.7)
463.05	462.62	462.83	462.62	462.83	N+ (462.13)
	470.09	470.09	470.09	470.09	O+ (470.118, 470.31, 470.53)
	478.4	478.4	478.4	478.4	N+ (478.813)
486.05					H (486.13)
				486.89	N2+ (486.715),
	492.83	493.04	492.83	492.83	
500.22	500.22	500.22	500.22	500.22	N+ (500.14, 500.27, 500.51)
517.48	518.11		518.11	518.11	
	565.72				
567.57			567.78	567.78	N+ (567.6, 567.95)
	580.31	580.31	580.31	580.31	
	589.11	589.11	589.11	589.11	Na (588.99,589.59)
593.8					
			616.13	616.13	Na (616.07)
656.4	656.4	656.4	656.4	656.4	H (656.27)
679.33	679.33	679.33	679.33	679.33	
	694.04	694.04	694.04	694.04	K (693.87)
744.45			744.64		
747.12	746.93		746.93	747.12	N (746.83)
755.3	755.3	755.3	755.3	755.3	
	766.65	766.84	766.65	766.65	K (766.49)
	770.05	770.05	770.05	770.05	K(769.89)
777.38	777.38	777.38	777.38	777.38	O (777.53)
			786.75	786.75	
795.14			794.95	794.95	O (795.08)
			809.04	809.04	
		819.17	819.35	819.35	N (818.48, 818.802)
	827.41				
844.88	844.88		844.88	844.88	O+ (844.62, 844.63, 844.67)
863.24			863.6	863.6	
868.43			868.61	868.43	N (868.02, 868.34, 868.61, 868.74)

Table 1 Various peaks assignment from the LIBS spectra of (a) ambient air (b) KBr pellet (c) AN + KBr pellet.

AIR	KBr	AP (NH_4ClO_4)			Element (NIST)
		Trial 1	Trial 2	Trial 3	
		374.58	374.36	374.58	N3+ (374.75), O3+(374.48),
				382.04	Cl+ (382.02, 382.7)
			393.21	393.21	N2+ (393.85)
399.33	399.11	399.11	399.33	399.11	N+ (399.5), N2+ (399.86)
	404.34	404.34	404.34	404.34	K (404.414)
	413.26	413.05		413.26	O+ (413.28)
	418.26	418.26	418.26		O+ (418.54, 418.97)
424.32	422.59	422.59	422.37		N+ (422.77)
	430.6		426.27		Cl (426.45)
		430.6	430.6		O+ (430.28, 430.36)
				438.15	Cl+ (438.97,437.99)
444.39	444.39	444.39	444.39		O+ (444.7, 444.8), N+ (444.7)
463.05	462.62	462.62	462.62	462.62	N+ (462.13)
	470.09	470.09	470.09	470.09	O+ (470.118, 470.31, 470.53)
	478.4	478.4	478.4	478.4	N+ (478.813) , Cl+ (478.132)
			481.38		Cl+ (481.006,481.947)
486.05					H (486.13), N2+ (486.715),
	492.83	492.83	492.83	493.04	
500.22	500.22	500.22	500.22	500.22	N+ (500.14, 500.27, 500.51)
517.48	518.11		517.9		
	565.72				
567.57			567.57	568.4	N+ (567.6, 567.95)
	580.31	580.31	580.31	580.31	
	589.11	589.11	589.11	589.72	Na(588.99, 589.59)
593.8					
				616.13	N (616.07)
656.4	656.4	656.4	656.4	656.4	H (656.27)
679.33	679.33	679.33	679.33	679.33	
			691.3		
	694.04	694.04	694.04	694.04	K (693.87)
				716.01	
744.45		744.64	744.45	744.64	N (744.22)
747.12	746.93		746.93	747.12	N (746.83)
755.3	755.3	755.3	755.3		
	766.65	766.65	766.65	766.65	K (766.49)
	770.05	770.05	770.05		K (769.89)
777.38	777.38	777.38	777.38	777.38	O (777.53)
795.14			795.14		O (795.08)
			809.04		
		819.17	819.35	819.53	N (818.48, 818.802)
			821.92		N (821.63)
	827.41		827.59		
844.88	844.88	844.88	844.88	844.88	O+ (844.62, 844.63, 844.67)
863.24		863.6	863.42		
868.43		868.43	868.43	868.61	N (868.02, 868.34, 868.61, 868.74)

Table 2 Various peaks assignment from the LIBS spectra of (a) ambient air (b) KBr pellet (c) AP + KBr pellet.

Stoichiometric Analysis of AP and AN

The H_α line (656.6 nm) was stronger in AN compared to AP and both were much stronger than that of KBR. The Oxygen line (at 777.38 nm) is a triplet and was not resolved in our case due to the insufficient resolution of spectrometer, which was ~1.5 nm. Nitrogen at 747 nm is also a triplet but the spectrometer was able to resolve in this case. The compositional analysis was done using the ratio of Oxygen peak at 777.38 nm and Nitrogen triplet peaks N_1, N_2, N_3 (742.54 nm, 744.64 nm, 747.12 nm). The intensity I_i of a spectral line occurring between two levels of the species **'i'** in the plasma is given by [3]:

$$I_i = C(g_i A_i / \lambda_i) \exp\left(-\frac{E_{up} - E_{low}}{KT}\right)$$

where $\boldsymbol{C}$ is $\frac{hcN_0}{4\pi Z}$, $\boldsymbol{h}$ is Planck's constant, $\boldsymbol{Z}$ is the partition function, N_0 is the initial number of atoms, $\boldsymbol{c}$ is the velocity of light, $\boldsymbol{g_i}$ is the statistical weight, $\boldsymbol{A}$ is the transition probability, $\boldsymbol{\lambda}$ is the wavelength of emission, $\boldsymbol{E}$ is the energy, and $\boldsymbol{T}$ is the plasma temperature, $\boldsymbol{K}$ is Boltzmann constant. The subscript **'i'** corresponds to the different peaks (at different wavelengths) being analyzed. Local thermodynamic equilibrium (LTE) has been assumed to prevail in the plasma so that a Boltzmann distribution is established among the bound energy levels. The plasma temperature $\boldsymbol{T}$ alters rapidly with time during the plasma evolution but LTE implies that a definite $\boldsymbol{T}$ can describe the plasma during the short time window when a spectrum is recorded. The areas under the Oxygen and Nitrogen peaks were calculated and then divided by corresponding '$\boldsymbol{gA}$' values. Three different ratios are calculated corresponding to the peaks of nitrogen at N_1 (742.54 nm), N_2 (744.64 nm), and N_3 (747.12 nm).

Table 3 summarizes the calculations and the results obtained for various concentrations of AP and AN. We found that the O (777.38)/N_1(742.54) ratio provided good agreement with the actual stoichiometric value for AP, and O(777.38)/N_3(747.12) for AN. The molecular formula of 'AN' is NH_4NO_3 and 'AP' is NH_4ClO_4 indicating that the stoichiometric ratios of O/N is 4 in AP and 1.5 in AN. The values presented in the table were averaged over ten different measurements where the input pulse energy was varied. It is evident that for 1.25 % and 2.5% doping (by weight %) yielded excellent agreement with the actual stoichiometric ratios. We had also performed the measurements with varying concentrations of AP and AN (5%, 10%, 20%, 40%, 75 %) and the ratios were once more in excellent agreement with the actual stoichiometric ratios, within the experimental error. We could also achieve small crystals of AN and the data obtained with those pure AN also indicate an excellent agreement of the experimental stoichiometric ratio with the actual ratio. Rai et al. [32] showed that for nitro-compounds O_1/N_2 ratio gives a correction indication of the actual stoichiometric ratio and identified different nitro compounds [10]. The major advantage of our work is that we had used a simple collection geometry consisting of a CCD spectrometer instead of a gated ICCD and spectrometer combination.

That only a particular ratio (O/N_1 or O/N_3) gives an accurate indication of actual stoichiometry in this case and is dissimilar for different compounds [32] needs to be investigated further. Of all the three Nitrogen peaks, N_1 has the lowest intensity (area under the curve) and N_3 has the highest intensity (area under the curve). It could be possible that to achieve better results (a) the denominator (N_3) had to be large for AN, with stoichiometric ratio of 1.5, and (b) the denominator had to be small for AP, with a stoichiometric ratio of 4, which was true in our case. We repeated the same experiment with a higher resolution spectrometer (MAYA, Ocean Optics, with a resolution of ~0.038 nm) to perceive the effect of resolution. Our initial data proved that the ratios were matching within the experimental error of ~15%. Detailed analyses are in progress. We are also collecting the data using an ICCD (ANDOR, istar DH734) coupled to a Mechelle spectrograph (ANDOR, ME5000) with gating facility and will try to compare the non-gated data with that of gated data. The effect of matrix presence/absence on the results is also being thoroughly investigated.

Sample(s)	Oxygen / Nitrogen peaks ratio			
	Stoichiometry	O (777.38) / N_1 (742.54)	O (777.38) / N_2 (744.64)	O (777.38) / N_3 (747.12)
AP + KBr matrix (25 mg in 20g)	4	5.11	1.89	1.49
AP + KBr matrix (50 mg in 20 g)		4.94	1.97	1.54
AN + KBr matrix (25 mg)	1.5	5.37	2.11	1.48
AN + KBr matrix (50mg)		5.71	2.21	1.64
Pure AN crystal		2.10	2.04	1.56

Table 3 Stoichiometric ratios of AP and AN calculated from the LIBS data.

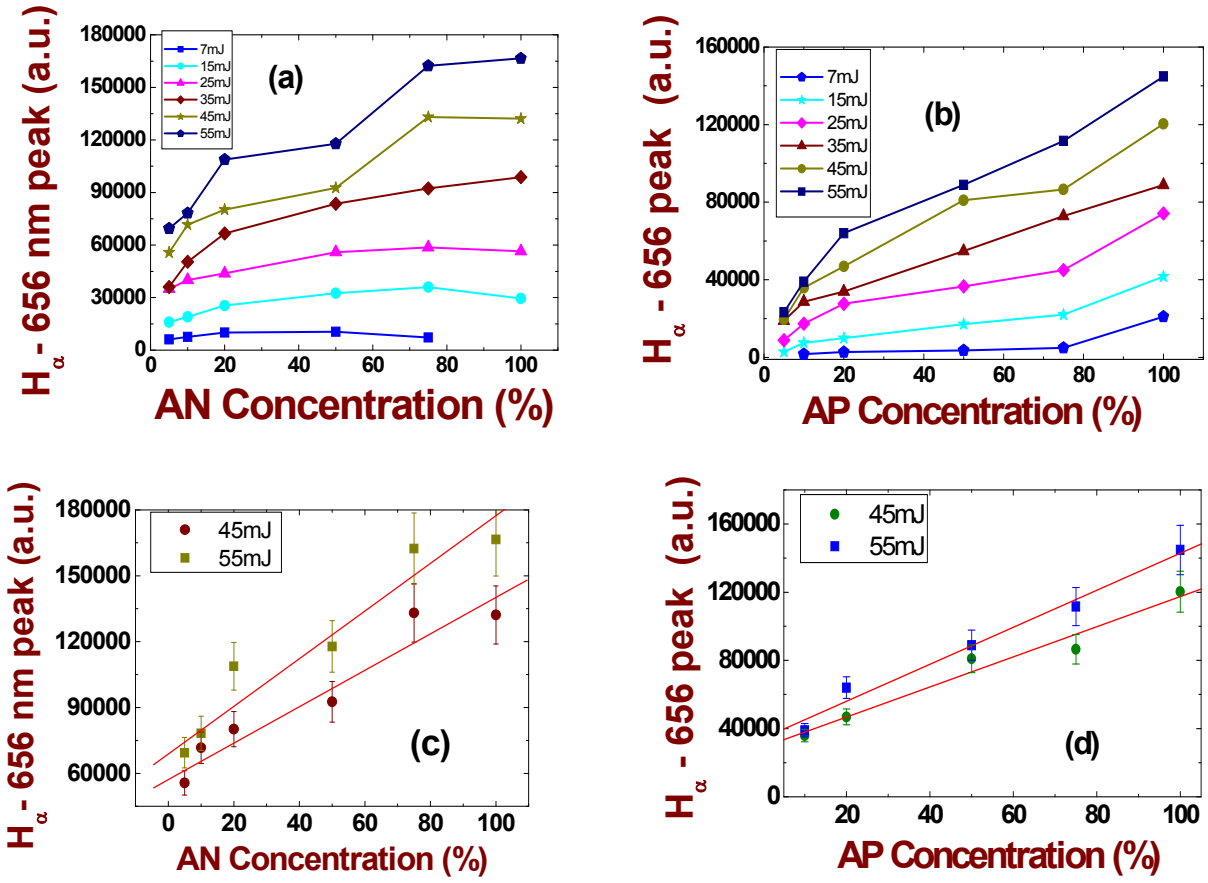

Figure 4 Variation of H_α line (656.4 nm) with varying concentration recorded at different energies of nanosecond laser pulses. (a) AN (b) AP. Linear dependence of the H_α peak versus concentration for (a) AN at higher energies (b) AP at higher energies.

Concentration dependent LIBS studies of AP and AN

AP and AN were taken with varying percentage ranging from 5 % to 100 % in KBr matrix. Calibration study (variation of $\mathbf{H_\alpha}$ peak intensity) was performed with different input pulse energies. Figures 4(a) and 4(b) depict the variation of $\mathbf{H_\alpha}$ intensity as a function of concentration for AN and AP, respectively. The input pulse energy increased from the bottom curve (~7 mJ) to the topmost curve (~55 mJ). The solid lines in these graphs are only a guide to the eye. The following conclusions can be drawn from the calibration data obtained: (a) For higher energies the change was pretty much linear, (b) for lower energies, except the 100% point, the dependence was again linear. A linear increment obtained for the $\mathbf{H_\alpha}$ line (656.6 nm) through a fit is plotted in figures 4(c) and 4(d) for AN and AP, respectively. This behavior is in agreement with that reported in literature [32]. We could also record the spectra of AP and AN crystals (typically few mm long) and the data is presented in figure 5. It is obvious that the pump (532 nm) peak dominated in spite of using filters. However, we could still resolve several peaks of **O, N, N^+, N^{2+}, Cl^+, H_α,** etc. Table 4 presents the summary of all the peaks identified. One can categorize the various peak intensities and their ratios for arriving at a reasonable strategy to distinguish these materials from other nitro-compounds using simple analysis.

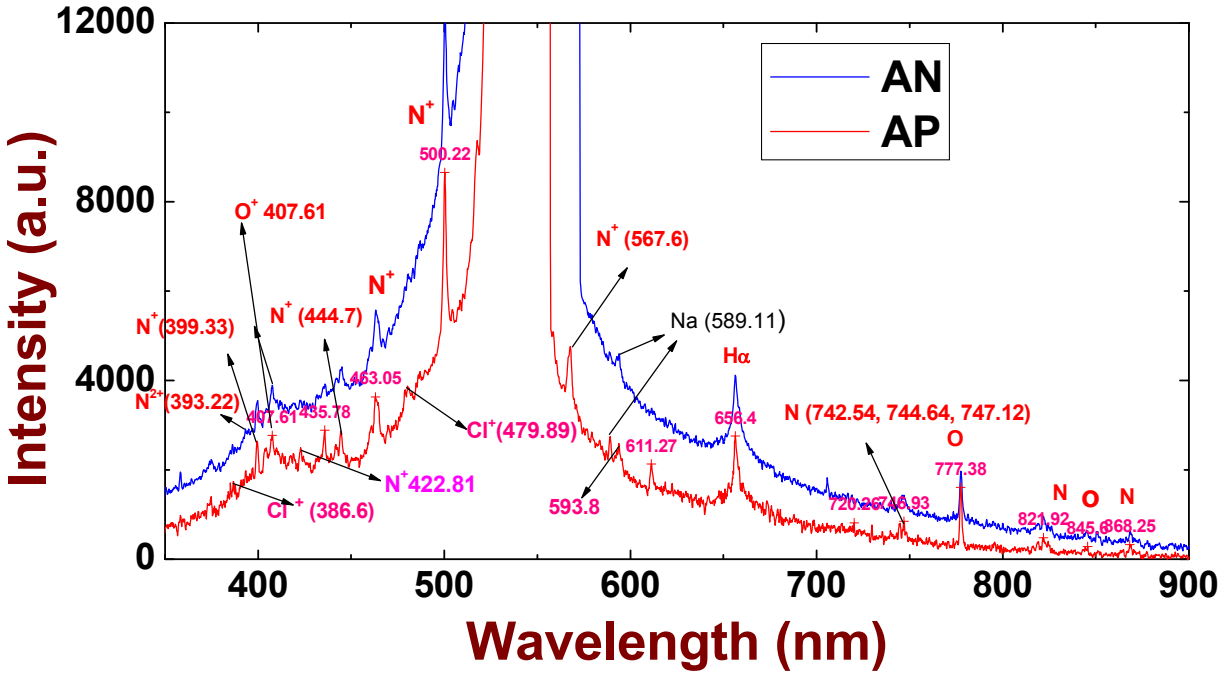

Figure 5 LIBS spectra of single crystals AP (lower curve) and AN (upper curve).

4.CONCLUSIONS

LIBS spectra of AP and AN have been recorded using nanosecond pulses and a non-gated spectrometer. The Oxygen to Nitrogen ratios were found to be 4.94 & 5.11 (O/N_1) for AP and 1.64 & 1.47 (O/N_3) for AN, which are in excellent agreement with the actual stoichiometric ratios of 4 and 1.5, respectively. Such analyses provide an opportunity to discriminate these compounds from other nitro-based compounds. We have also performed the calibration studies of AP and AN in a KBr matrix and recorded the LIBS spectra of pure AP and AN. Our future studies will focus on (a) collecting the gated LIBS data using an ICCD (b) compare the gated and non-gated data for arriving at a suitable strategy for identification of these compounds.

Peaks observed	AP	AN	NIST Database [33]
393.3	Y	N	N^{2+} (393.85)
399.3	Y	Y	N^{+} (399.5), N2+ (399.86)
386.6	Y	N	Cl^{+} (386.083)
444.7	Y	Y	N^{+} (444.7)
500.22	Y	Y	N^{+} (500.14, 500.27, 500.51)
567.6	Y	Y	N^{+} (567.6, 567.95)
407.61	Y	Y	O^{+} (407.58)
589.11	Y	Y	Na (588.99, 589.59)
744.6, 747.12	Y	Y	N (Triplet) (742.364, 744.229 , 746.831
656	Y	Y	H_{α} (656.4)
777.38	Y	Y	O (777.19, 777.41, 777.53)
821.92	Y	Y	N (822.31)
845.06	Y	Y	O^{+} (844.62, 844.63, 844.67)
868.25	Y	Y	N (868.02, 868.34, 868.61, 868.74)

Table 4 various peak assignments from the pure AP and AN LIBS spectra.

5. ACKNOWLEDGEMENTS

We thank Dr. Anuj Verghese for providing us the samples of AP and AN. We also thank DRDO, India for financial support.

6. REFERENCES

[1] *"Laser-Induced Breakdown Spectroscopy (LIBS). Fundamentals and Applications,"* A.W. Miziolek, V. Palleschi, and I. Schechter, Editors, Cambridge University Press, New York, 2006.

[2] *"Laser-Induced Breakdown Spectroscopy,"* J.P. Singh & S.N. Thakur, Elsevier Science B. V., Amsterdam, The Netherlands (2007)

[3] *"Handbook of Laser-Induced Breakdown Spectroscopy,"* D.A. Cremers, L.J. Radziemski,John Wiley & sons Ltd., UK (2006).

[4] D. A. Rusak, B. C. Castle, B. W. Smith, and J. D. Winefordner, "Fundamentals and applications of laser-induced breakdown spectroscopy," Crit. Rev. Anal. Chem. **27,** 257-290 (1997).

[5] R.S. Harmon, F.C. De Lucia, A.W. Miziolek, K.L. McNesby, R.A. Walters, and P.D. French, "Laser-induced breakdown spectroscopy (LIBS): an emerging field-portable sensor technology for real-time, in-situ geochemical and environmental analysis," Geochem. Explor. Envi. Analy. **5**, 21-28 (2005).

[6] R. Grönlund, M. Lundqvist, and S. Svanberg, "Remote imaging laser-induced breakdown spectroscopy and remote cultural heritage ablative cleaning," Opt. Lett. **30,** 2882-2884(2005).

[7] M. Sabasi and R. Russo, eds., 4th International Conference on Laser Induced Plasma Spectroscopy and Applications (LIBS 2006) Special Issue Spectrochim. Acta, Part B, **62**, 1285-1618(2006).

[8] F. C. De Lucia, Jr., R. S. Harmon, K. L. McNesby, R. J. Winkel, Jr., and A. W. Miziolek, "Laser-Induced Breakdown Spectroscopy Analysis of Energetic Materials," Appl. Opt. **42**, 6148-6152 (2003).

[9] R. S. Harmon, F. C. DeLucia, Jr., A. LaPointe, R. J. Winkel, Jr., and A. W. Miziolek, "LIBS for landmine detection and discrimination," Anal. Bioanal. Chem. **385,** 1140-1148 (2006).

[10] C. A. Munson, F. C. De Lucia, Jr., T. Piehler, K. L. McNesby, and A. W. Miziolek, "Investigation of statistics strategies for improving the discriminating power of laser-induced breakdown spectroscopy for chemical and biological warfare agent simulants," Spectrochim. Acta Part B, **60,** 1217-1224 (2005).

[11] A. C. Samuels, F. C. DeLucia Jr., K. L. McNesby, and A. W. Miziolek, "Laser-induced breakdown spectroscopy of bacterial spores, molds, pollens, and protein: initial studies of discrimination potential," Appl. Opt. **42,** 6205-6209 (2003).

[12] S. J. Rehse, J. Diedrich, and S. Palchaudhuri, "Identification and discrimination of Pseudomonas aeruginosa bacteria grown in blood and bile by laser-induced breakdown spectroscopy," Spectrochim. Acta, Part B, **62,** 1169-1176 (2007).
[13] J. Diedrich, S. J. Rehse, and S. Palchaudhuri, "Pathogenic Escherichia coli strain discrimination using laser-induced breakdown spectroscopy," J. Appl. Phys. **102**, 014702 (2007).
[14] J. D. Hybl, G. A. Lithgow, and S. G. Buckley, "Laser-induced breakdown spectroscopy detection and classification of biological aerosols," Appl. Spectrosc. **57**, 1207-1215 (2003).
[15] E. Gibb-Snyder, B. Gullett, S. Ryan, L. Oudejans, and A. Touati, "Development of size-selective sampling of Bacillus anthracis surrogate spores from simulated building air intake mixtures for analysis via laser-induced breakdown spectroscopy," Appl. Spectrosc. **60,** 860-870 (2006).
[16] B. Bousquet, J. B. Sirven, and L. Canioni, "Towards quantitative laser-induced breakdown spectroscopy analysis of soil samples," Spectrochim. Acta, Part B**62,** 1582-1589 (2007).
[17] F. C. DeLucia, Jr., A. C. Samuels, R. S. Harmon, R. A. Walters, K. L. McNesby, A. LaPointe, R. J. Winkel, Jr., and A. W. Miziolek, "Laser-induced breakdown spectroscopy (LIBS): a promising versatile chemical sensor technology for hazardous material detection," IEEE Sens. J. **5,** 681-689(2005).
[18] V. Lazic, A. Palucci, S. Jovicevic, C. Poggi, and E. Buono, "Analysis of explosive and other organic residues by laser induced breakdown spectroscopy," Spectrochimica Acta Part B: Atomic Spectroscopy **64(10)**, 1028-1039 (2009).
[19] C.A. Munson, J.L. Gottfried, F.C. De Lucia Jr., K.L. McNesby, and A.W. Miziolek, "Laser-based Detection Methods of Explosives," in *Counterterrorist Detection Techniques of Explosives*, J. Yinon, Ed. (Elsevier, Amsterdam), 279–321 (2007).
[20] Y. Dikmelik, C. McEnnis, J.B. Spicer, "Femtosecond and nanosecond laser-induced breakdown spectroscopy of trinitrotoluene," Opt. Express **16(8)**, 5332-5337 (2008).
[21] V.I. Babushok, F.C. Delucia Jr, P.J. Dagdigian, J.L. Gottfried, C.A. Munson, M.J. Nusca, A.W. Miziolek, "Kinetic modeling study of the laser-induced plasma plume of cyclotrimethylenetriamine (RDX)", Spectrochimica Acta Part B, **62**, 1321-1328 (2007).
[22] J. L. Gottfried, F. C. De Lucia, Jr., C. A. Munson, and A. W. Miziolek, "Laser-induced breakdown spectroscopy for detection of explosives residues: A review of recent advances, challenges, and future prospects," Analytical and Bioanalytical Chemistry **395(2)**, 283-300 (2009).
[23] C. López-Moreno, S. Palanco, J.J. Laserna, F. DeLucia Jr, A.W. Miziolek, J. Rose, R.A. Walters, and A.I. Whitehouse "Test of stand of detection breakdown spectroscopy sensor for the detection of explosive residues on solid surfaces," J. Anal. At. Spectrom. **21**, 55-60 (2006).
[24] J. L. Gottfried, F. C. De Lucia, Jr., C. A. Munson, and A. W. Miziolek, "Strategies for residue explosives detection using laser-induced breakdown spectroscopy," J. Anal. At. Spectrom. **23**, 205-216 (2008).
[25] J. L. Gottfried, F. C. De Lucia, Jr, C. A. Munson, and A. W. Miziolek, "Standoff detection of chemical and biological threats using laser-induced breakdown spectroscopy," Appl. Spectrosc. **62**, 353-363 (2008).
[26] M. Bengtsson, R. Gronlund, M. Lundqvist, A. Larsson, S. Kroll, and S. Svanberg, "Remote laser-induced breakdown spectroscopy for the detection and removal of salt on metal and polymeric surfaces," Appl. Spectrosc. **60**, 1188-1191(2006).
[27] H. L. Xu, G. Méjean, W. Liu, Y. Kamali, J. F. Daigle, A. Azarm, P. T. Simard, P. Mathieu, G. Roy, J. R. Simard, and S. L. Chin, "Remote detection of similar biological materials using femtosecond filament-induced breakdown spectroscopy," Appl. Phys. B**, 87,** 151-156 (2007).
[28] Ph. Rohwetter, J. Yu, G. Mejean, K. Stemaszczyk, E.S.J. Kasparian, J.P. Wolf, L. Woste "Remote LIBS with ultrashort pulses: characteristics in picosecond and femtosecond regimes", J. Anal. At. Spectrom. **19**, 437-444 (2004).
[29] V.I. Babushok, F.C. Delucia Jr, J.L. Gottfried, C.A. Munson, A.W. Miziolek, "Double pulse laser ablation and plasma: Laser induced breakdown spectroscopy signal enhancement," Spectrochim. Acta Part B, **61,** 999–1014 (2006).
[30] J.L. Gottfried, F.C. De Lucia, Jr., C.A. Munson, A.W. Miziolek, "Double-pulse standoff laser-induced breakdown spectroscopy for versatile hazardous materials detection," Spectrochim. Acta, Part B **62,** 1405-1411 (2007).
[31] S.K. Rai, A.K. Rai, S.N. Thakur, "Identification of nitro-compounds with LIBS", Appl. Phys. B **91**,645 (2008).
[32] D. Díaz, D.W. Hahn, A. Molina, "Laser induced breakdown spectroscopy (LIBS) for detection of ammonium nitrates in solids," Proc. SPIE **7303**, 73031E (2009).
[33] http://physics.nist.gov/PhysRefData/ASD.